

1 **Oceland: A conceptual model for ocean-land-atmosphere interactions based**
2 **on water balance equations**

3 Luca Schmidt^a, Cathy Hohenegger^a

4 ^a *Max Planck Institute for Meteorology, Hamburg*

5 *Corresponding author:* Luca Schmidt, luca.schmidt@mpimet.mpg.de

6 ABSTRACT: The spatial distribution of precipitation is often misrepresented by General Cir-
7 culation Models (GCM). In particular, precipitation tends to be underestimated over land and
8 overestimated over ocean. One obstacle to resolving this longstanding issue is the lack of a general
9 understanding of land-ocean-atmosphere interactions. More precisely, we do not have a funda-
10 mental theory that tells us which processes or physical quantities determine the partitioning of
11 precipitation between land and ocean. In this study, we investigate whether large-scale constraints
12 on this partitioning exist by using a conceptual box model based on water balance equations. With
13 a small number of empirical but physically motivated parametrizations of the water balance com-
14 ponents, we construct a set of coupled ordinary differential equations which describe the dynamical
15 behaviour of the water vapour content of land and ocean atmospheres as well as the soil moisture
16 content of land. We compute the equilibrium solution of this land-ocean-atmosphere system and
17 analyze the sensitivity of the equilibrium state to model parameter choices. The results show that
18 the ratio of mean land and ocean precipitation rates is primarily controlled by a scale-dependent
19 atmospheric moisture transport parameter, the land fraction, and the permanent wilting point of
20 the soil. We further demonstrate how the proposed model can be adapted for applications on
21 both global and local scales to model, where the latter is useful to study e.g. island precipitation
22 enhancement. For a global scale model configuration with one ocean and one land domain, we
23 show that the precipitation ratio is constrained to a range between zero and one and are able to
24 explain this behavior based on the underlying equations and the fundamental property of land to
25 loose water through runoff.

26 1. Introduction

27 As human beings, we have a great interest in how Earth's climate and its change over time
28 influence living conditions on the land surface. An important question in this respect is how much
29 of the water that evaporates from the Earth's surface will precipitate over land as opposed to over
30 the ocean. Unfortunately, even sophisticated General Circulation Models such as those evaluated
31 in the Coupled Model Intercomparison Project have longstanding difficulties reproducing observed
32 spatial patterns of precipitation as well as their frequency and intensity, especially in the Tropics
33 where precipitation amounts are high (Fiedler et al. (2020) and references therein). However, more
34 fundamentally, we are lacking a theoretical framework in which the partitioning of precipitation
35 between land and ocean can be explained and analyzed with respect to its dependence on properties
36 of the system which may or may not change over time. For instance, is the partitioning sensitive to
37 land size? Do surface characteristics such as soil type matter or is it rather atmospheric conditions
38 that dominate the behavior? It is the aim of this study to introduce a conceptual water balance model
39 that reduces the complexity of the real world to a small number of physical processes that are key
40 for understanding the precipitation partitioning. By investigating the sensitivity of the modelled
41 precipitation partitioning to a variation of the model parameter values across the parameter space,
42 this study can serve as a starting point for filling the gap of theoretical understanding described
43 above.

44 Traditionally, hydrologists separate the Earth's hydrological cycle into an atmospheric and a
45 terrestrial branch (e.g. Peixóto and Oort (1983)). The atmospheric water balance describes the
46 rate of change of the atmospheric water content at a given location, with surface evapotranspiration
47 (ET) and moisture flux convergence as inputs and precipitation as output. Similarly, the terrestrial
48 water balance considers the change of soil moisture content with precipitation as input and ET and
49 runoff as outputs. Evapotranspiration and precipitation are the links that connect the two branches
50 of the cycle. Since we aim at understanding the precipitation partitioning between land and ocean,
51 it is convenient to choose a different perspective and think about an ocean and a land branch of
52 the water cycle instead. The land and ocean branch are then linked through horizontal moisture
53 flux convergence, i.e. moisture transport between land and ocean atmospheres, and through runoff
54 from the soil to the ocean.

The land branch in isolation has been studied intensively since the 1950s. In a pioneering land-atmosphere interaction study by Budyko and Drozdov (1953), the authors established the notion that an airstream that traverses a region imports atmospheric moisture at the windward contour of the region and exports moisture at the leeward contour. The amount of exported moisture depends on the windward moisture value and on subsequent moistening or drying of the air as it traverses the region. The net change of moisture in the air is determined by the relative magnitude of mean precipitation (drying) and mean ET from the surface (moistening). In this one-dimensional framework known as the Budyko model, precipitation can be expressed as a sum of two components: water molecules that were advected from outside the region and ones that previously evaporated from the surface inside the region. Due to the assumption of a well-mixed boundary layer, molecules of different origin cannot be discriminated but their relative contribution to precipitation can be described by the so-called moisture exchange coefficient. This coefficient describes the ratio of total precipitation to advected precipitation and was the first of several similar water recycling coefficients that were used to quantify the dependence of precipitation in a given region on moisture import from an outside environment relative to local moisture recycling through ET. Important studies of this kind which used observations to estimate the water balance components include Brubaker et al. (1993), who adapted the Budyko model for a two-dimensional land region and investigated the annual cycle of precipitation recycling in four innercontinental areas and Eltahir and Bras (1994), who studied moisture recycling in the Amazon by likewise working in two dimensions and allowing for a horizontally heterogeneous precipitation and evapotranspiration field. A comprehensive review of the different adaptations of Budyko's framework and their individual caveats can be found in Burde and Zangvil (2001). A prominent shortcoming of the early approaches are that the recycling ratio depends strongly on the size of the region of interest, with larger areas leading to higher and smaller areas to lower recycling ratios. Ent et al. (2010) circumvented this limitation by producing global maps of precipitation recycling where recycled water is defined as previously evaporated from any point on the land surface and advected water as evaporated from any point on the ocean surface. All these studies show that precipitation recycling contributes significantly to land precipitation, especially in hotspot regions of land-atmosphere interactions such as the Sahel region, the Amazon or mountainous regions in Asia.

An alternative to estimating the water balance components from observations is to use analytical parametrizations. In water-limited areas, ET is a function of the relative soil moisture saturation as described by e.g. Manabe (1969) or more recently updated in Seneviratne et al. (2010). Inserting such an expression for ET into the Budyko recycling framework turns the total precipitation into a function of relative soil moisture saturation and mean rate of advected precipitation as well as a set of parameters such as wind speed, the spatial extent of the region and potential ET. The variability of the latter parameters introduce considerable randomness to precipitation in the real world and limit the utility of the Budyko model when being fixed to a constant value. Rodriguez-Iturbe et al. (1991) and Entekhabi et al. (1992) addressed this issue by modulating mean parametric environmental conditions with Gaussian white noise. They found a surprising behavior when solving their model for equilibrium rain rates: The stronger the variability of environmental conditions, the clearer two pronounced modes of equilibrium solutions emerged. The system had a high probability to reside in either a very dry state near or below the permanent wilting point of the soil or in a very wet state near soil saturation. At the same time, intermediate soil moisture states were only rarely attained. These results suggested an explanation for droughts in continental areas.

What are the physical mechanisms that make precipitation dependent on soil moisture? Broadly speaking, two lines of arguments were developed to answer this question. The first one predicts a mostly positive feedback between precipitation and soil moisture, arguing that the enhanced latent heat flux over wet soils favors precipitating convection either through direct water input that can be recycled (e.g. Zangvil et al. (1993)) or by destabilizing the vertical profiles of the air aloft and thus favouring precipitating convection (Schär et al. (1999), Findell and Eltahir (2003) and Hohenegger et al. (2009), the latter pointing out that the sign of the feedback is also dependent on model resolution). The second line of argument explains soil moisture-precipitation feedbacks based on mesoscale circulations that develop due to different Bowen ratios of wet and dry soil patches Segal and Arritt (1992). Such circulations drive convective systems from rather moist to rather dry surface areas and contribute to a homogenization of soil moisture (Lynn et al. (1998), Hohenegger and Stevens (2018)). However, Froidevaux et al. (2014) found that synoptic background winds can displace convective air from drier soils, where convection was initiated, to wetter soils where the atmospheric conditions favor the onset of precipitation. Hence, the sign of the soil moisture feedback related to mesoscale processes is unclear.

115 Lastly, the circulation argument has direct implications for our initial question regarding the
116 partitioning of precipitation between ocean and land. Especially in the context of Tropical islands,
117 several studies show that precipitation is enhanced over land due to sea-breezes induced by dif-
118 ferential heating between the land surface and surrounding ocean (Qian (2008) and Cronin et al.
119 (2015)). Even though island precipitation enhancement is often linked to energy balance which
120 is not considered in this work, other factors such as island size (Sobel et al. (2011), Cronin et al.
121 (2015), Wang and Sobel (2017) and Ulrich and Bellon (2019)) and background wind speed (Sobel
122 et al. (2011), Wang and Sobel (2017)) seem to influence the precipitation partitioning, too. We
123 will return to these aspects in the last part of this paper.

124 2. Model description

125 Explanation for proofreading: Red text means comments and questions. Blue and orange text is
126 used when different versions of a sentence/paragraph are proposed.

127 Somewhere I would like to put a basic statement of our modelling objective, i.e. modelling
128 water fluxes and their partitioning between land and ocean. Maybe this could be stated here as an
129 introductory sentence to the model description. In this case, read the blue text below. Alternatively,
130 it could be said in the end of the introduction. Or, yet another alternative: I could eliminate the
131 heading "Design goals" and just have the text below directly after the heading "Model description".
132 Then, the orange version would apply.

133 a. Design goals

134 Conceptual models do not try to explain natural processes in an exact, quantitative manner.
135 Rather, they aim at helping us understand the dominant physical relationships that give rise to a
136 certain natural phenomenon. These dominant factors often get modulated and thereby obscured by
137 a plethora of other processes acting simultaneously in the real world and are therefore difficult to
138 disentangle in observations or simulations with sophisticated climate models. Conceptual models
139 can provide clarity at the expense of realism and with the danger of missing out on relevant physical
140 processes. The successful development of a conceptual model is therefore an iterative process that
141 begins with the most basic assumptions and ends when "the model is only as elaborate as it needs
142 to be to capture the essence of a particular source of complexity, but is no more elaborate than

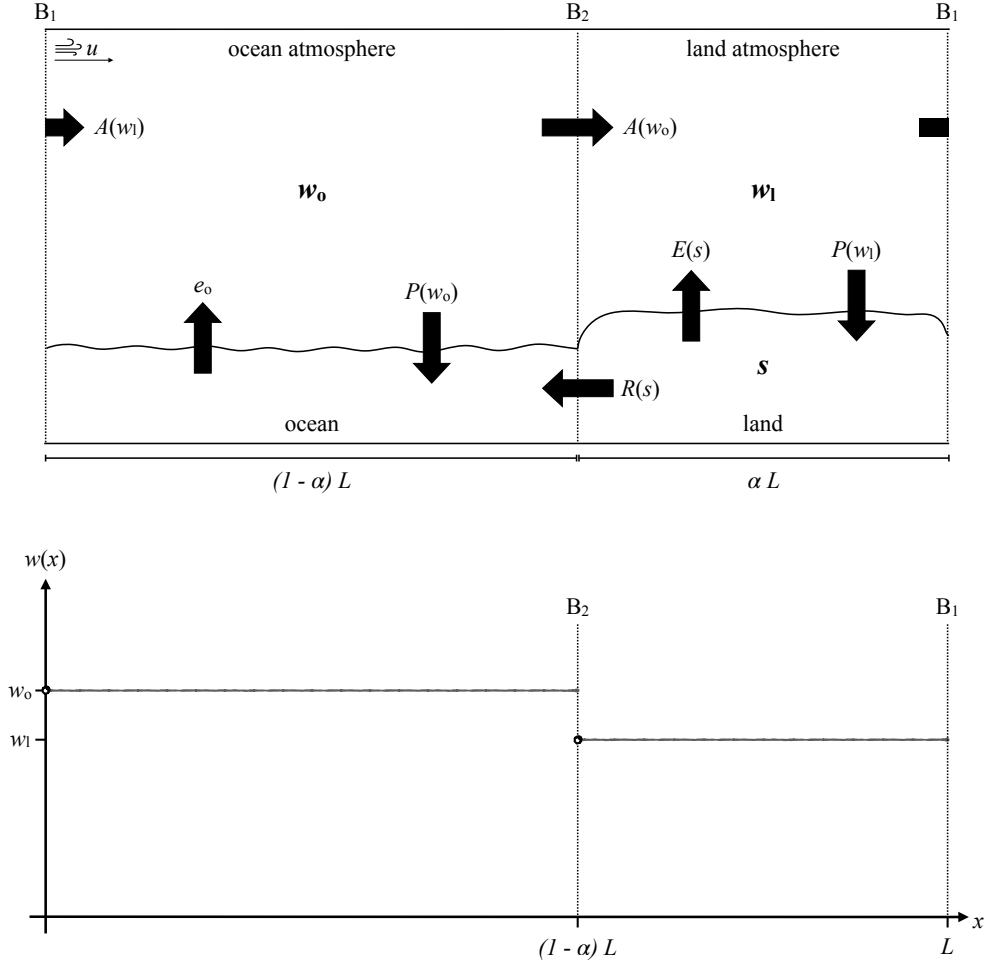


FIG. 1. Closed model sketch and water vapor pass distribution.

143 this", as Held (2005) puts it. Version 1: It is our hope that the model proposed in this study
 144 meets this balance and that the assumptions and choices that were made in the model development
 145 process become clear. Version 2: The complexity we address in this work is the partitioning of
 146 precipitation and other water fluxes between land and ocean and its particular source might be
 147 the fundamental properties of the two surface types and how they interact with each other and the
 148 atmosphere to constrain the exchange of water.

149 *b. Closed model setup*

150 We propose a 2D box model as sketched in the top panel of Figure 1, which consists of an ocean
 151 domain, denoted by subscript ‘o’, and a land domain, denoted by subscript ‘l’. Actually, how

many dimensions do we have? We don't resolve neither the x - nor y -direction explicitly. In this sense, we would have only the time-dimension, but we aren't even interested in time evolution as such but only the equilibrium. On the other hand, we implicitly assume the existence of spatial dimensions x and y by placing the boxes in a specific way. And the model extent in x -direction is even explicitly in the equations with L ... Each of the two domains contains a ground box at the bottom and an atmospheric box aloft. However, this spatial arrangement is only relevant in so far as we are interested in the water fluxes across the boundaries connecting any two boxes. We assume that all fluxes can be expressed as functions of the mean moisture states of the model boxes so that an explicit dependence on the spatial variables (x, y) is obsolete. This choice trades some realism for the ease of working with ordinary differential equations (ODEs) instead of partial differential equations (PDEs).

The mean moisture states of the model boxes represent their water content. For atmospheric boxes, we use the mean integrated water vapour mass w in mm, and for the land box the unitless mean relative soil moisture saturation s to describe the state. As the ocean is considered fully saturated at all times, the influence of the ocean state on fluxes is constant in time and can be prescribed in the form of a parameter. This means that the full information on the moisture state of the model at any given moment in time t is given by the set of state variables $\{w_o(t), w_l(t), s(t)\}$.

We limit the modelled water exchange between boxes to the following four flux types, denoted by arrows in Fig. 1: Evapotranspiration E from ground to atmosphere, precipitation P from atmosphere to ground, advection A between the atmospheric boxes and runoff R from land to ocean. Expressions for these fluxes as functions of the state variables are provided in Section d.

It is important to note that we assume the model to have closed boundaries at the top of the atmosphere and the bottom of the ground boxes, while periodic boundary conditions are used in horizontal direction. This is, the model topologically resembles the walls of a cylinder and the right boundary of the land domain connects to the left boundary of the ocean domain. A constant mean background wind is introduced to facilitate advection and gives the atmospheric moisture transport a fixed directionality. **Motivated by a net easterly wind in the Tropics, ...?**

Lastly, the relative size of the ocean and land domain is set by the land fraction parameter α . The spatial extent of the land in x -direction is given by αL , where L denotes the full model length. Conversely, the ocean has a horizontal extent of $(1 - \alpha)L$.

182 *c. Water balance equations*

183 To a good approximation, the total amount of water is conserved within the tropical band. If we
 184 further assume that the mean water holding capacity of the atmosphere does not vary significantly
 185 over time, we can apply these properties of the tropics to our model and formulate a set of coupled
 186 differential equations that describe the rate of change of the water content in each of our model
 187 boxes. **Maybe, we don't want to make a clear reference to the Tropics at this point. In this case,**
 188 **this paragraph can be reformulated in a more neutral way, where water conservation and constant**
 189 **water holding capacity are just general assumptions.** As we assume the moisture state of the ocean
 190 to be constant in time, the number of equations reduces by one and we are left with the following
 191 expressions for the changes in soil moisture saturation and land and ocean mean water vapour
 192 passes:

$$\frac{ds}{dt} = \frac{1}{nz_r} [P(w_l) - R(s, w_l) - E(s)] \quad (1)$$

$$\frac{dw_l}{dt} = E(s) - P(w_l) + A_l(w_l, w_o) \quad (2)$$

$$\frac{dw_o}{dt} = e_o - P(w_o) + A_o(w_l, w_o). \quad (3)$$

193 The water transfer terms P , R , E , e_o , A_l and A_o are expressed as mean fluxes in mm/day.
 194 The advection terms A_l and A_o refer to *net* advection rate into the land and ocean atmosphere,
 195 respectively, and are positive for a net moisture import and negative for net moisture export. Ocean
 196 evaporation rate e_o in mm/day, dimensionless soil porosity n and hydrologically active soil depth
 197 z_r in mm are constant parameters of the system.

198 *d. Parametrizations*

199 While the conservation of water is a rather fundamental condition, there are no simple, fun-
 200 damental laws governing the water fluxes between the model boxes. Instead, we need to draw
 201 inspiration from existing literature that provides empirical relationships between the flux quantities
 202 and our model state variables.

203 Bretherton et al. (2004) provide such an empirical parametrization for oceanic, tropical precipi-
 204 tation rate in mm/day as a function of the mean water vapor pass,

$$P(w) = \exp \left[a \left(\frac{w}{w_{\text{sat}}} - b \right) \right]. \quad (4)$$

The parametrization introduces three parameters, two empirical dimensionless parameters $a \approx 15.6$ and $b \approx 0.6$ and the saturated water vapor pass w_{sat} in mm. Lacking a corresponding expression for tropical land regions, we will make the explicit assumption that the oceanic precipitation formulation can also be applied to land atmospheres. This assumption has major implications for the results presented in Section 4 as will be discussed in greater detail later. **It might be worth it to spend a day or two looking at ERA5 data over(tropical) land and check if we see at least a similar relationship between water vapor pass and precipitation. In the end, this assumption is critical to our conclusion about PR<1 in the closed model. If there is absolutely no correlation between P and w over land, then we would have to think a lot harder about how to sell this. If I was the reviewer, I would probably pick on this and ask if we did a sanity check before making this assumption..** Furthermore, the same saturation water vapor pass is assumed over land and over ocean, implying similar energetic conditions across the entire model domain.

Runoff gets parametrized as the fraction R_f of precipitation that does not infiltrate the soil but returns to the ocean in the form of surface or sub-surface currents. This approach was, for instance, used in Rodriguez-Iturbe et al. (1991). The runoff fraction,

$$R_f(s) = \epsilon s^r, \quad (5)$$

contains two empirical dimensionless parameters $\epsilon \approx 1$ and $r \approx 2$. It tells us that runoff intensifies as the soil moistens. The complete expression for the runoff rate reads

$$R(s, w_1) = R_f(s)P(w_1), \quad (6)$$

but it proves to be convenient to combine precipitation and runoff in Eqn. (1) to $P(w_1) - R(s, w_1) = P(w_1)\Phi(s)$, where we introduced the infiltration function $\Phi(s) = 1 - R_f = 1 - \epsilon s^r$. Note, that this parametrisation assumes that runoff discharge happens uniformly across the land domain and that its water does not participate in any secondary processes that could moisten the soil.

The qualitative dependence of evapotranspiration (ET) on soil moisture saturation is long-known and was first introduced by Budyko (1956). ET is close to zero for soil moisture saturation values

below the permanent wilting point, $s < s_{\text{pwp}}$, increases approximately linearly in a transition range between the permanent wilting point and a critical value close to the field capacity, $s_{\text{pwp}} < s < s_{\text{fc}}$ and reaches a plateau for higher s -values, $s > s_{\text{fc}}$, where evapotranspiration is nearly constant. Is it ok to write it like this or should I rather explain that it is no longer water-limited beyond s_{fc} ? ...Because technically, a higher temperature could lead to higher evapotranspiration. We just don't model this energy-relationship. For computational convenience, we parametrize this sometimes piecewise defined behaviour by the following smooth equivalent:

$$E(s) = \frac{E_p}{2} \left[\tanh \left(10 \left(s - \frac{s_{\text{pwp}} + s_{\text{fc}}}{2} \right) \right) + 1 \right]. \quad (7)$$

The potential evapotranspiration E_p signifies the value of the plateau beyond s_{fc} . This parametrization implies that the entire land box is either covered by a single vegetation type or that a combination of vegetation types can be modelled by means of an effective mean value of s_{pwp} , s_{fc} and E_p . Furthermore, the model does not consider energy conservation, so that an even higher evapotranspiration beyond E_p due to an enhanced radiative energy input is precluded by design.

It remains to find expressions for the *mean net* advection rates into the land and ocean atmospheres, hereafter mean land/ocean advection rates. The net total advection flux into a given box is the difference between the moisture entering and leaving the box per unit time. It can be written as the windward boundary water vapour pass times wind speed minus the analogous term at the leeward boundary of the box,

$$A_{\text{tot}} = (w_{\text{in}} - w_{\text{out}})u. \quad (8)$$

The sketch in the bottom panel of Figure 1 illustrates the assumed water vapour pass distribution across the full model domain. Since we only have two boxes and periodic boundary conditions, the total net advection rate A_{tot} into the land and ocean atmospheres are identical in magnitude but with opposite signs. If the ocean has a net advective outflux, then the land atmosphere gains this moisture as net advective influx. By applying Eqn. (8) to the w -distribution in Figure [***] for the land and ocean atmosphere boxes, respectively, and translating the obtained total net advection fluxes into *mean* advection rates per unit land/ocean length, we obtain

$$A_1 = \frac{(w_o - w_l)u}{\alpha L} \quad (9)$$

TABLE 1. Parameter ranges for closed model Monte Carlo simulations with uniform sampling.

Parameter	Minimum	Maximum	Range choice motivated by
s_{pwp}	0.2	0.54	Hagemann and Stacke (2015)
s_{fc}	0.5	0.84	Hagemann and Stacke (2015)
e_{p} [mm/day]	4.1	4.5	Rodriguez-Iturbe et al. (1991)
nZ_{T} [mm]	90.0	110.0	Rodriguez-Iturbe et al. (1991)
e_{o} [mm/day]	2.8	3.2	C. Hohenegger, private communications
ϵ	0.9	1.1	Rodriguez-Iturbe et al. (1991)
r	2.0	2.0	fixed due to computational method, Rodriguez-Iturbe et al. (1991)
a	11.4	15.6	Bretherton et al. (2004)
b	0.522	0.603	Bretherton et al. (2004)
w_{sat} [mm]	65.0	80.0	Bretherton et al. (2004)
α	0.0	1.0	full possible range
u [m/s]	1.0	10.0	needs more research/thoughts
L [km]	1000.0	40000.0	needs more research/thoughts
$\tau = u/L$ [day $^{-1}$]	0.00216	0.864	computed from extreme u and L

and

$$A_{\text{o}} = -\frac{(w_{\text{o}} - w_{\text{l}})u}{(1 - \alpha)L}, \quad (10)$$

where α and L are the land fraction and full model length, respectively, as introduced in Section b.

With these parametrizations, the model has a total of 14 free parameters which we can reduce to 12 if we treat nZ_{T} in mm as one combined parameter and $\tau = u/L$ in day $^{-1}$ as a characteristic rate of atmospheric transport. Table 1 provides sensible ranges for the 12 parameters. These ranges are used to constrain the precipitation ratio across the parameter space and test the sensitivity of the model results to parameter variations.

3. Evaluation methods

In this section, we present the analysis methods that are employed to evaluate the model behavior and assess the sensitivity of the precipitation ratio to a variation of the model parameters.

The focus of the present study lies on the properties of equilibrium states of the modelled system. The equilibrium solution to the model equations (1) to (3) has to be found numerically. We use the `DynamicalSystems.jl` library from Datseris (2018) to find all roots of the model equations and determine whether each root represents a stable or unstable fixed point of the system. With the equilibrium soil moisture and water vapour pass values obtained in this way, we can compute all fluxes and flux ratios of interest using the parametrizations introduced in Section 2.d.

Adopting an agnostic view on the plausibility of each combination of parameter values from the ranges given in Tab. 1, we are confronted with a 12-dimensional parameter space with uniform probability distribution. A general assessment of the sensitivity of equilibrium states and, in particular, the precipitation ratio to a variation of the model parameters requires a sampling of the full parameter space. In order to minimize computational costs and avoid systematic biases, this sampling is done in a random manner. We perform $n = 10000$ model simulations for randomly chosen combinations of parameter values, each yielding a corresponding fixed point.

Having obtained a sufficiently large dataset in this way, the sensitivity of a computed quantity Q such as the precipitation ratio to a given parameter p can be visually and numerically evaluated with scatter plots. A random distribution of data points across the entire range of p indicates insensitivity of Q to a variation in p . In this case, the choice of a certain p -value has no predictive power for the value of Q . In contrast, a scatter plot distribution where data points cluster in a non-uniform way points to a stronger sensitivity. We can construct a more objective measures of sensitivity from scatter plots by subdividing the range of p into N equally spaced bins, labelled by $i = 1, \dots, N$, and quantifying how much the mean value of Q in each bin, μ_i , differs from the total mean across the full range of p , μ_{tot} . Following this approach, the overall sensitivity S of Q to a variation in p is expressed as,

$$S = \frac{1}{N} \sum_{i=1}^N |\mu_i - \mu_{\text{tot}}|. \quad (11)$$

If Q is insensitive to p , all bin means μ_i lie close to μ_{tot} and the value of S is small. If instead, Q is very sensitive to p , then the point cloud will be diverted towards higher or lower values than the mean in most bins and S has a relatively high value.

4. Closed model results

The results presented in this section are based on the data of 10000 simulations of the closed model (CM) which randomly sampled the parameter space as explained in Section 3, each yielding the equilibrium solution for a unique point in the parameter space provided in Table 1. The obtained dataset will henceforth be referred to as "CM data". The section is organised in two parts. First, we discuss basic features of the model and their implications for the partitioning of precipitation

294 between land and ocean. Second, we examine to which parameters the precipitation ratio is most
295 sensitive and which physical arguments explain the individual relationships.

296 *a. Basic model behaviour*

297 From a first visual inspection, it is clear that the equilibrium states and resulting equilibrium
298 mean water fluxes P_1 , P_o , E_1 , R , A_1 and A_o , show a strong dependence on the choice of land fraction
299 α . It is therefore instructive to discuss basic features of the model output with the help of scatter
300 plots of the water fluxes over α . These plots are provided in Figure 2. Similar figures that show the
301 dependence on other parameters are provided in appendix [***]. Note, that the ocean advection
302 rate A_o has a negative value in all runs and is therefore multiplied by -1 in order to obtain the
303 absolute values which are more easily compared to the other fluxes.

304 All mean fluxes are functions of the equilibrium solutions to Eqns. (1) - (3) and therefore depend
305 implicitly on the choice of parameter values. Expressions for the fluxes as explicit, analytical
306 functions of α or other parameters are cumbersome to find or may not exist. We therefore explain
307 the observed features with qualitative, physical arguments rather than with mathematical rigor.

308 To begin with, Figure 2 shows that all equilibrium mean fluxes lie in the range $[0, e_o]$, with
309 $e_o \approx 3$ mm/day. With the exception of $-A_o$, maximum values are attained for $\alpha \rightarrow 0$ and the fluxes
310 decrease monotonically but in nonlinear ways with increasing land fraction. To understand these
311 general features and draw first conclusions for the partitioning of precipitation between land and
312 ocean, two observations about the mean land advection rate A_1 (bottom left panel) and runoff rate
313 R (middle right panel) are key:

- 314 1. Land advection is positive (ocean advection is negative) for all equilibrium states.
- 315 2. The mean land advection rate is identical to mean runoff rate, i.e. $A_1 = R$.

316 The first observation implies a clear directionality of the atmospheric water transport for the
317 system in equilibrium. Moisture is supplied *by* the ocean atmosphere *to* the land atmosphere.
318 This directionality of advection sets the upper limit of the precipitation ratio in the following way:
319 From Eq. (9) follows that a positive mean land advection rate requires the ocean atmosphere to be
320 moister than the land atmosphere, i.e. $w_o > w_1$. As we assume that the same parametrization holds
321 for precipitation over ocean and land, it further follows that $P_o > P_1$ and, consequently,

$$PR = \frac{P_1}{P_o} < 1. \quad (12)$$

Should a discussion of possible pathways for $PR > 1$ come already here or later?

The second observation helps to explain why the unidirectionality of moisture transport from ocean to land exists. In order to sustain a constant, nonzero equilibrium soil moisture value, $s > 0$, land precipitation needs to balance the water loss of the soil through evapotranspiration and runoff. While the amount of precipitation that is turned into evapotranspiration resides in a self-sustaining recycling loop between land atmosphere and soil, runoff is irretrievably lost to the ocean. Its share in the precipitation balance needs to be supplied to the land atmosphere in the form of advection,

$$P_1 = E_1 + R = E_1 + A_1. \quad (13)$$

If we imagine a system without advection, e.g. because the land and ocean atmosphere were separated by an impenetrable barrier, runoff would continuously reduce the soil moisture saturation and with it the evapotranspiration and precipitation fluxes. Eventually, the system would attain the trivial equilibrium solution $\{s = 0, w_1 = 0\}$. On the ocean side of this hypothetical system, equilibrium conditions would be rather moist with w_o such that $P_o(w_o) = e_o$. We conclude that it is the fundamental property of land to lose water in the form of runoff that requires an atmospheric moisture flux from ocean to land for any nontrivial equilibrium solution.

Based on these insights, we can also understand why no individual water flux can exceed the value of the ocean evaporation. Ocean precipitation needs to be smaller than e_o because some of the evaporated water gets advected by the land atmosphere and is no longer available for precipitation. Over land, we already established that $P_1 < P_o$ with the consequence that $P_1 < e_o$. The land precipitation is partitioned into E_1 and R so that each of these two fluxes must be smaller than e_o . Land advection is constrained by $A_1 = P_1 - E_1 < e_o$ and ocean advection is limited to $A_o \lesssim e_o$ as the ocean atmosphere can only export as much moisture as it receives from the ocean surface minus the amount that precipitates. At the same time, A_o cannot attain e_o as the basic requirement for advection is $w_o > w_1 > 0$ which comes along with nonzero ocean precipitation.

As we increase the land fraction from $\alpha = 0$ to $\alpha = 1$, all fluxes except A_o decrease in magnitude. The dependence of our system on α enters our model equations through the mean advection rates

347 A_1 and A_o . The same amount of exchanged water per unit time $(w_o - w_1)u$, that solely depends
 348 on the atmospheric moisture contents and wind speed, translates to an amount per time and unit
 349 length for the ocean with factor $1/((1 - \alpha)L)$ and for land with factor $1/(\alpha L)$. Combining Eqns.
 350 (2) and (3) under the equilibrium assumption of vanishing time derivatives, we can formulate the
 351 equilibrium condition,

$$e_o = P_o(w_o) + \frac{\alpha}{1 - \alpha} \underbrace{[P_1(w_1) - E_1(s)]}_{R(s)}. \quad (14)$$

352 Equation (14) tells us, that the constant ocean evaporation rate needs to balance the sum of ocean
 353 precipitation rate and the difference between land precipitation and ET that is multiplied by an
 354 α -dependent term. This term, $\alpha/(1 - \alpha)$, goes to zero for $\alpha \rightarrow 0$ and increases monotonically until
 355 it diverges to infinity for $\alpha \rightarrow 1$. As α increases, the equilibrium state needs to adjust by either
 356 decreasing w_o , w_1 or s . However, due to the coupling between all three state variables, a decrease in
 357 only one of the state variables does not result in a new equilibrium state. Instead, all state variables
 358 have to decrease together so that the new equilibrium state is dryer in all boxes (except the ocean).
 359 We can also understand this more intuitively: Despite the constant mean evaporation rate of the
 360 ocean, the total moisture input from the ocean is reduced as the land surface increases and the
 361 ocean surface shrinks. A lesser amount of water is available to sustain the soil moisture value of
 362 a larger land box. Consequently, starting from a rather moist state when the ocean and its total
 363 water input into the atmosphere are large, the entire system undergoes drying with increasing land
 364 fraction. This process terminates when the entire model domain is covered by land ($\alpha = 1$). Just
 365 before this point, when α is close to 1, a tiny ocean atmosphere exports almost the entire moisture
 366 that gets evaporated from the ocean surface, $(1 - \alpha)L|A_o| \lesssim e_o$, but this amount is just sufficient to
 367 keep the large land atmosphere at a moisture value $w_1 \gtrsim 0$ so that the resulting land precipitation
 368 stabilises the land at a very small soil moisture value $s \gtrsim 0$.

369 Do you think I should say anything about the specific shape of the relationships in Fig. 2? I
 370 don't have very satisfying, easy physical reasons to explain them. It seems to me like the shapes
 371 are simply a result of the interplay of the different nonlinear parametrisations that we use. I could
 372 probably reason about them in a similar style as the discussion about the upper limit e_o for the

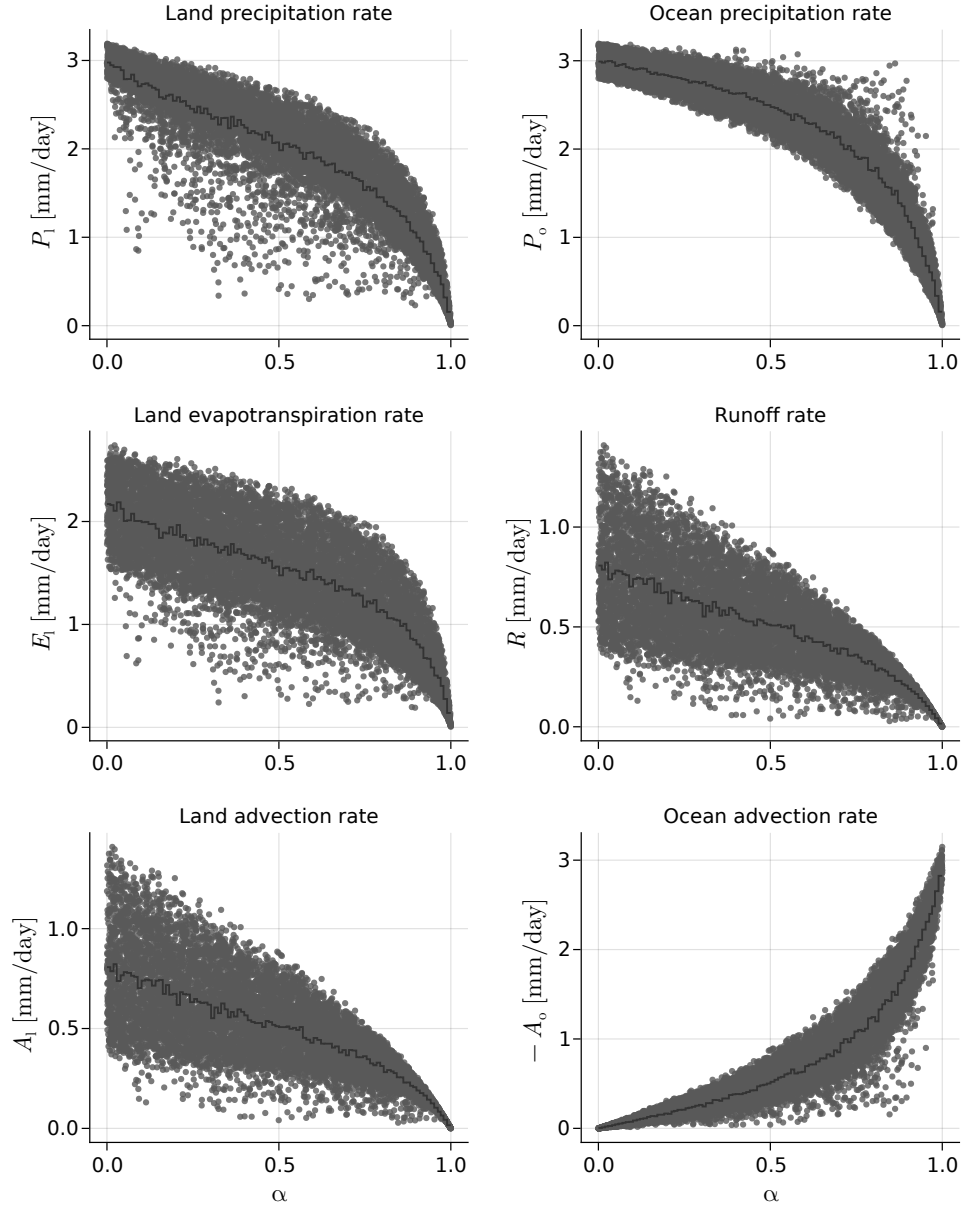


FIG. 2. Mean water fluxes computed from the equilibrium states of 10000 closed model runs with randomly sampled parameter values and plotted over land fraction α . The dark grey line shows the mean values of bins of 100 consecutive α -values. The negative ocean advection rate A_o reflects a net transport of water out of the ocean and into the land atmosphere. Multiplication by -1 simplifies the comparison of its magnitude with the other flux quantities.

fluxes, i.e. by showing an equation and then discussing what needs to happen if we increase α by a bit in different α regimes. But this seems very boring and pointless to me.

380 *b. Parameter sensitivity of PR*

381 Building on the preceding general description of the model behavior, we now draw our attention
 382 to the sensitivity of the precipitation ratio with respect to a variation of different model parameters.
 383 Three parameters stand out in having a particularly strong impact on PR : Land fraction α ,
 384 atmospheric moisture transport parameter τ and permanent wilting point s_{pwp} . We discuss the
 385 underlying relationships using the same CM data as before.

386 **Land fraction α :** Figure 3 shows a scatter plot of PR values over α . Despite considerable
 387 spread in PR , we can see that $PR \rightarrow 1$ for both limits, $\alpha \rightarrow 0$ and $\alpha \rightarrow 1$. This reflects very
 388 similar moisture conditions in the two atmospheres when α is extreme. Knowing that $w_o > w_l$
 389 for all equilibrium states, it follows that PR will only decrease if $\Delta w = w_o - w_l$ increases. As has
 390 been discussed in the preceding section, the system's equilibrium states for a tiny land domain are
 391 relatively moist. For $\alpha \rightarrow 0$, a large Δw cannot be sustained since the resulting advection amount
 392 $\Delta w u$ would translate to a large land advection rate, $\Delta w u / (\alpha L)$, that would immediately moisten
 393 the land atmosphere and assimilate w_o and w_l . On the other end of the range, when the ocean is
 394 tiny, i.e. $\alpha \rightarrow 1$, large moisture differences are likewise impossible: This time, Δw is limited by
 395 the total amount of water that enters the system through the ocean surface. The ocean atmosphere
 396 cannot export more water than it receives. Therefore, the total amount of evaporated water sets
 397 the upper limit for advection, $\Delta w u < (1 - \alpha) L e_o$. This amount decreases with increasing α , so
 398 that Δw needs to decrease with it. Moreover, Δw needs to stay below this limit since the ocean
 399 atmosphere has to stay moister than the land atmosphere to facilitate advection in the first place.

400 Along the mid- α range, PR decreases until it reaches a minimum beyond which the ratio
 401 increases again. This behaviour is somewhat concealed by the large spread in PR for intermediate
 402 land fractions but is both visible in the means of bins of 100 consecutive α values (dark grey line)
 403 and in graphs for which all parameters except α were kept fixed (not shown). A mathematically
 404 rigorous analysis of $PR(\alpha)$ in this range and, in particular, the location of the minimum is difficult
 405 due to the lack of an analytical expression for the relationship between precipitation ratio and land
 406 fraction. We can write,

$$PR(\alpha) = \frac{P_l(\alpha)}{P_o(\alpha)} = \frac{E_l(s) + \frac{(w_o - w_l)u}{\alpha L}}{e_o - \frac{(w_o - w_l)u}{(1 - \alpha)L}}, \quad (15)$$

but we may not overlook the fact that our state variables are implicit functions of α , too, i.e. $s(\alpha)$, $w_o(\alpha)$ and $w_l(\alpha)$. Even though we don't know the analytical form of these state variable dependencies, Eqn. (3) gives a useful indication of why the precipitation ratio should decrease for small but increasing α and why it should increase again as α approaches one. This indication lies in the factors $f = 1/\alpha$ and $g = 1/(1 - \alpha)$ in the land and ocean advection rates, respectively. Assuming that the system resides in an equilibrium state for some α close to zero, a small increase in α would lead to a rather strong drop in the land advection rate (strong negative slope of f at low α) compared to the rather mild increase in the magnitude of ocean advection (weakly positive slope of g at low α)...

I stopped here because I wondered if it makes sense to explain the shape of $PR(\alpha)$ in such great detail. Maybe all this could be described in a much simpler way by starting from total moisture input rather than mean rates. The argument would go something like this: increasing land = generally less water available to the circulation in the system. Consequently, the moisture state as a whole must become drier, i.e. all state variables decrease but at different rates. Land precip (and with it w_l) decrease both through a reduction of E_l and a rather sharp drop in A_l due to factor f . Ocean precip only decreases by slight increase of $-A_o$. For large α the system is already in a rather dry state. E_l decreases only slightly with decreasing s and impact of f is less strong. For ocean precip, the opposite is true. Here, g plays a stronger role now and increases the ocean advection rate strongly. In the end, the interplay of the different nonlinear parametrisations make the behaviour of PR asymmetric around $\alpha = 0.5$ and hard to understand in detail.

Atmospheric rate of transport τ : The ratio between mean horizontal wind speed and spatial extent of the model, $\tau = u/L$, is a measure for the efficiency with which moisture is transported across the model atmosphere. Its inverse value, τ^{-1} , corresponds to the time that an air parcel would need to travel across the full domain length L . In the advection terms of Eqn. (2) and (3), τ appears as the rate at which moisture is moved across the boundaries between the two atmospheric boxes. It has therefore major implications for the ability of advection to assimilate the moisture conditions over ocean and land. A very small value of τ , i.e. a low rate of transport, corresponds to a combination of large domain size and low wind speed while a small domain and strong wind result in a very large value of τ . Assuming a fixed land fraction α , a larger moisture difference Δw is needed to move the same total amount of water across a box boundaries when the rate of

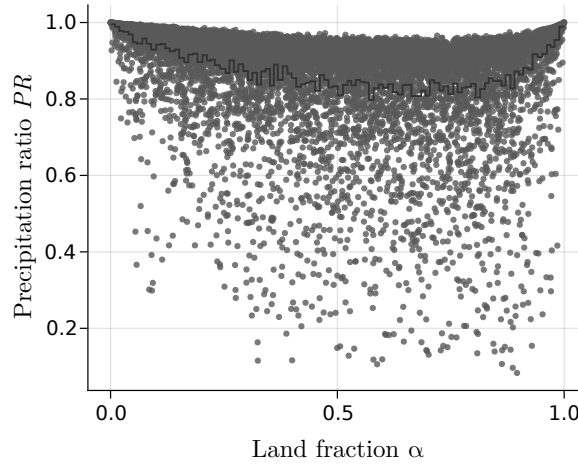


FIG. 3. Smile plot

transport is small, compared to when it is large. Except for the special cases of extreme land fractions, $\alpha \rightarrow \{0, 1\}$, where α enforces very similar moisture conditions over land and ocean, it is primarily τ that sets the moisture difference which is needed to attain the equilibrium state. This dominant role is illustrated in Figure 4 which shows the scatter plot of precipitation ratio over τ . While we already assessed that α sets the overall upper limit of PR , Fig. 4 shows that τ sets the overall lower bound. It explains the large spread for PR values in the mid- α range in Figure 3, where the efficiency of atmospheric moisture transport is particularly important. Only high rates of transport enable the system to attain an equilibrium state with rather similar moisture conditions over land and ocean. For instance, if $\tau > 0.4 \text{ day}^{-1}$, then PR stays above 0.8 regardless of the choice of values for other parameters. Note, that τ combines the information about both wind and spatial extent of the model. If one fixes one of the two, e.g. $L = 40000 \text{ km}$ to simulate the full Tropics along the equator, the physically sensible range of τ is limited. For example, in order to obtain a rate of transport larger than 0.4 day^{-1} , such a large L would require a minimum wind speed of 185 m/s , a value that lies beyond the highest wind speed ever measured on Earth. More realistic mean wind speed values for such a large domain could lie around 5 to 10 m/s (Needs to be checked! Maybe by looking at ERA5 data?) with corresponding rates of transport, $\tau \approx 0.01 - 0.02$. At these low values of τ , the spread of PR values is considerable which means that also other parameters have a substantial influence on the attained equilibrium state.

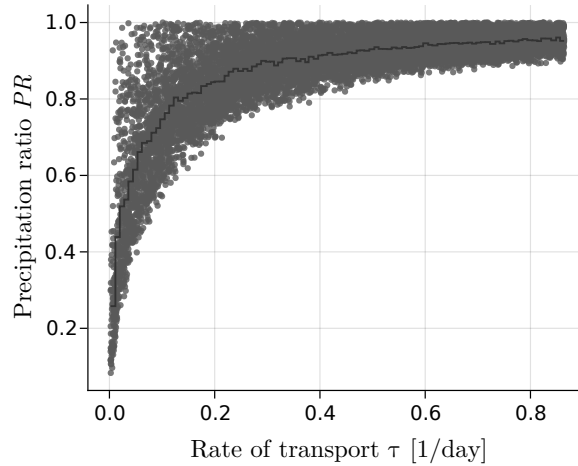


FIG. 4. τ -dependence

Permanent wilting point s_{pwp} : It takes work to extract water from the soil and the drier the soil, the more work is needed to facilitate evapotranspiration. Regardless of whether the land surface is bare or covered with vegetation, s_{pwp} is a characteristic property of the soil type which denotes the relative soil moisture saturation value below which practically no water can be extracted. The left panel of Figure 5 shows the parametrization function of evapotranspiration, $E_1(s)$, for different choices of the permanent wilting point. For instance, $s_{\text{pwp}} \approx 0.3$ might correspond to loam and $s_{\text{pwp}} \approx 0.5$ to clay (Hagemann and Stacke (2015)). In the evapotranspiration graphs, s_{pwp} determines the soil moisture value at which the curve transitions from $E_1 \approx 0$ to the regime of steeply increasing E_1 . Since the field capacity s_{fc} lies $\Delta s = 0.3$ higher than s_{pwp} for all relevant soil types, a change in s_{pwp} merely shifts the evapotranspiration graph along the s -direction, while its shape remains unchanged.

Figure 6 shows a negative trend of the precipitation ratio with increasing s_{pwp} for the performed model runs. The impact of soil type on the precipitation ratio is weaker than, for example, the impact of τ but it is nonetheless clearly visible and s_{pwp} represents the third most sensitive model parameter. To understand the dependence of PR on s_{pwp} , it is convenient to think of a system in equilibrium for some permanent wilting point, e.g. $s_{\text{pwp}} = 0.3$. The mean equilibrium soil moisture value in the CM data for $s_{\text{pwp}} = 0.3$ is $s = 0.43$. This initial state of the model is displayed as a blue dot in Figure 5. An abrupt increase of s_{pwp} to $s_{\text{pwp}} = 0.4$ leads to a significant drop of E_1 as illustrated by the first red arrow connecting the blue and green dot in the left panel of

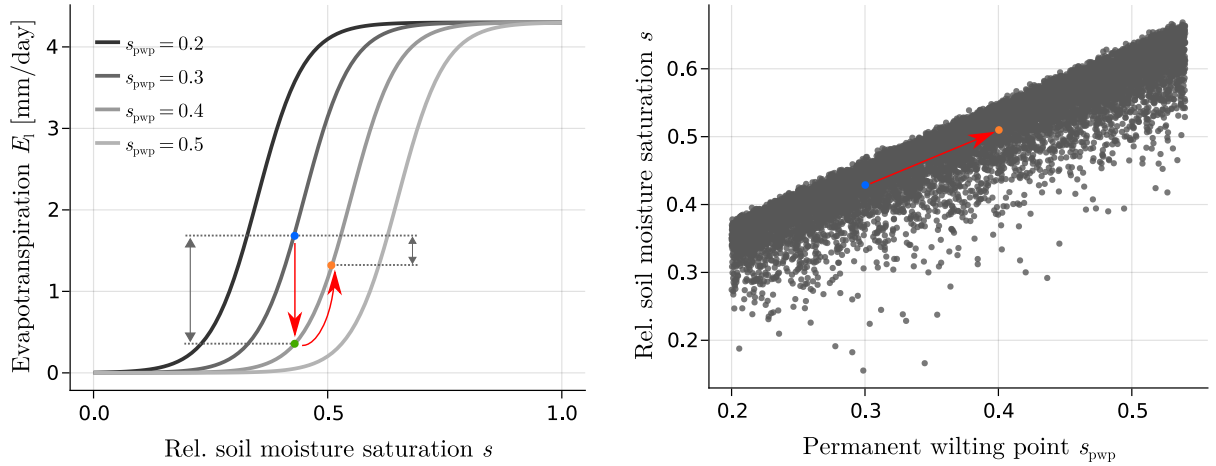


FIG. 5. Influence of an increase in s_{pwp} on the equilibrium state. Left: Higher values of s_{pwp} shift the graph of the E_l parametrization towards larger s . Right: Equilibrium values of the soil moisture saturation from CM data plotted over s_{pwp} values. In left panel, next to left black arrows will stand something like ΔE_{inst} for instantaneous ET-difference and next to the right black arrows ΔE_{eq} to denote the ET difference between old and new equilibrium state.

Fig. 5. The green dot represents a temporary state where the model is not in equilibrium because the state variables have not yet adapted to the new situation. At this point, the soil receives the same amount of precipitation but loses less water through evapotranspiration. As a result, the soil moistens. As time progresses, the system attains a new equilibrium state at a higher s value which is marked by the orange dot. This moistening of the soil is shown in the right panel of Fig. 5, where the equilibrium s values of the CM data are plotted over the corresponding values of s_{pwp} . However, as s increases, runoff and land advection rate increase, too. Assuming that $\tau/(\alpha L)$ is kept fixed, Δw has to increase to facilitate the increase of advection. The water that is supplied to the land atmosphere as advection is taken from the ocean atmosphere, where w_o decreases as a consequence. Hence, an increase in advection is only possible, if w_l decreases more strongly than w_o . The increase in R combined with a decrease in P_l is the reason why the new equilibrium state for $s_{pwp} = 0.4$ will have a moister soil but a lower evapotranspiration rate than the initial state for $s_{pwp} = 0.3$. The fact that w_l must decrease more strongly than w_o in the adaptation process is the reason why PR declines with increasing s_{pwp} .

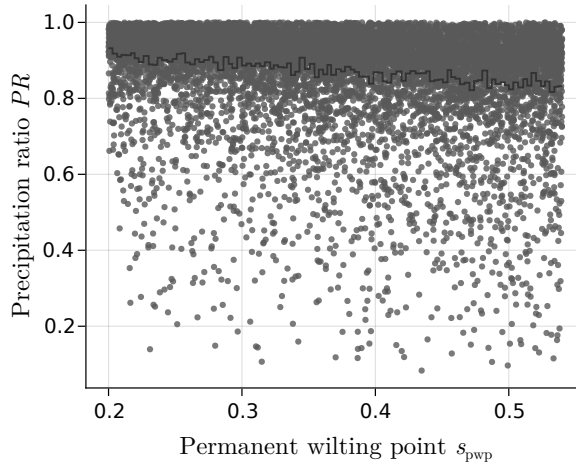


FIG. 6. s_{pwp} -dependence

5. Open model formulation

The closed model discussed so far can be applied to any system for which the total net advection is zero. Such conditions might be met in the real world when we look at very large scales, e.g. global domains such as the tropical band. However, in the case of more local, small scale phenomena, the net advection might not be zero and the situation is better captured by an open model configuration, where moisture inflow at the windward model boundary is a model parameter and no constraints apply to the moisture outflow at the leeward boundary. In this model configuration, the modelled domain can have a net advection larger or smaller than zero. In the following, we present the formalism and analysis of an open model with two oceanic domains and an island inbetween them.

a. Open model equations

The model equations for an open configuration are similar to the ones for the closed model. This time, four instead of three equations are needed as the system has now one more ocean domain. The meaning of the soil moisture variable s is unchanged, while a different notation is employed for the water content of the atmospheric boxes. The index $i = 1, 2, 3$ is used to denote the mean integrated water vapour pass w_i and net advection rate A_i of the first ocean atmosphere ($i = 1$), land atmosphere ($i = 2$) and second ocean atmosphere ($i = 3$), respectively. With this, the model equations read

$$\frac{ds}{dt} = \frac{1}{nz_r} [P(w_2) - R(s, w_2) - E(s)] \quad (16)$$

$$\frac{dw_1}{dt} = e_o - P(w_1) + A_1 \quad (17)$$

$$\frac{dw_2}{dt} = E(s) - P(w_2) + A_2 \quad (18)$$

$$\frac{dw_3}{dt} = e_o - P(w_3) + A_3, \quad (19)$$

with

$$A_i = \frac{(w_{i-1} - w_i)u}{L_i}. \quad (20)$$

Note, that a new parameter w_0 was introduced which denotes the boundary condition of the water vapor pass at the windward end of the model domain. It reflects the **synoptic scale?** conditions which the model is embedded in.

b. Open model results

- How the open model relaxes the condition that $PR < 1$ ($PR > 1$ only under certain conditions)
- The role of synoptic moisture conditions in the atmosphere
- Transforming the open model into the closed model

6. Discussion and summary

- Which conditions need to be met to end up with a precipitation ratio larger one?
- What are possible use cases for the models?
- What can the model(s) tell us and what not and why? (e.g. land distribution not representative for the Tropics)

525 *Acknowledgments.*

526 *Data availability statement.*

527 **References**

- 528 Bretherton, C. S., M. E. Peters, and L. E. Back, 2004: Relationships between water vapor path
529 and precipitation over the tropical oceans. *J. Climate*, **17**, 1517–1528, [https://doi.org/10.1175/](https://doi.org/10.1175/1520-0442(2004)017<1517:RBWVPA>2.0.CO;2)
530 1520-0442(2004)017<1517:RBWVPA>2.0.CO;2.
- 531 Brubaker, K. L., D. Entekhabi, and P. S. Eagleson, 1993: Estimation of continental precipita-
532 tion recycling. *Journal of Climate*, **6**, 1077–1089, [https://doi.org/10.1175/1520-0442\(1993\)](https://doi.org/10.1175/1520-0442(1993)006<1077:EOCPR>2.0.CO;2)
533 006<1077:EOCPR>2.0.CO;2, URL [https://journals.ametsoc.org/jcli/article/6/6/1077/39303/](https://journals.ametsoc.org/jcli/article/6/6/1077/39303/Estimation-of-Continental-Precipitation-Recycling)
534 Estimation-of-Continental-Precipitation-Recycling.
- 535 Budyko, M. I., 1956: *Heat balance of the Earth's surface*. U.S. Dept. of Commerce, Weather
536 Bureau.
- 537 Budyko, M. I., and O. A. Drozdov, 1953: Characteristics of the moisture circulation in the
538 atmosphere. **4**, 5–14.
- 539 Burde, G. I., and A. Zangvil, 2001: The estimation of regional precipitation recycling. part i:
540 Review of recycling models. *Journal of Climate*, **14** (12), 2497–2508, [https://doi.org/10.1175/](https://doi.org/10.1175/1520-0442(2001)014<2497:TEORPR>2.0.CO;2)
541 1520-0442(2001)014<2497:TEORPR>2.0.CO;2, URL [https://journals.ametsoc.org/jcli/article/](https://journals.ametsoc.org/jcli/article/14/12/2497/29526/The-Estimation-of-Regional-Precipitation-Recycling)
542 14/12/2497/29526/The-Estimation-of-Regional-Precipitation-Recycling.
- 543 Cronin, T. W., K. A. Emanuel, and P. Molnar, 2015: Island precipitation enhancement and
544 the diurnal cycle in radiative-convective equilibrium. **141** (689), 1017–1034, [https://doi.org/](https://doi.org/10.1002/qj.2443)
545 10.1002/qj.2443, URL <https://rmets.onlinelibrary.wiley.com/doi/abs/10.1002/qj.2443>.
- 546 Datseris, G., 2018: Dynamicalsystems.jl: A julia software library for chaos and nonlinear dynam-
547 ics. *Journal of Open Source Software*, **3**, 598, <https://doi.org/10.21105/joss.00598>.
- 548 Eltahir, E. a. B., and R. L. Bras, 1994: Precipitation recycling in the amazon basin. *Quarterly Jour-*
549 *nal of the Royal Meteorological Society*, **120**, 861–880, <https://doi.org/10.1002/qj.49712051806>,
550 URL <https://onlinelibrary.wiley.com/doi/abs/10.1002/qj.49712051806>.

Ent, R. J. v. d., H. H. G. Savenije, B. Schaefli, and S. C. Steele-Dunne, 2010: Origin and fate of atmospheric moisture over continents. *Water Resources Research*, **46** (9), <https://doi.org/10.1029/2010WR009127>, URL <https://agupubs.onlinelibrary.wiley.com/doi/abs/10.1029/2010WR009127>.

Entekhabi, D., I. Rodriguez-Iturbe, and R. L. Bras, 1992: Variability in large-scale water balance with land surface-atmosphere interaction. *Journal of Climate*, **5**, 798–813, [https://doi.org/10.1175/1520-0442\(1992\)005<0798:VILSWB>2.0.CO;2](https://doi.org/10.1175/1520-0442(1992)005<0798:VILSWB>2.0.CO;2), URL <https://journals.ametsoc.org/jcli/article/5/8/798/35919/Variability-in-Large-Scale-Water-Balance-with-Land>.

Fiedler, S., and Coauthors, 2020: Simulated tropical precipitation assessed across three major phases of the coupled model intercomparison project (CMIP). *Monthly Weather Review*, **148** (9), 3653–3680, <https://doi.org/10.1175/MWR-D-19-0404.1>.

Findell, K. L., and E. A. B. Eltahir, 2003: Atmospheric controls on soil moisture–boundary layer interactions. part i: Framework development. *Journal of Hydrometeorology*, **4** (3), 552–569, [https://doi.org/10.1175/1525-7541\(2003\)004<0552:ACOSML>2.0.CO;2](https://doi.org/10.1175/1525-7541(2003)004<0552:ACOSML>2.0.CO;2), URL <https://journals.ametsoc.org/jhm/article/4/3/552/68951/Atmospheric-Controls-on-Soil-Moisture-Boundary>.

Froidevaux, P., L. Schlemmer, J. Schmidli, W. Langhans, and C. Schär, 2014: Influence of the background wind on the local soil moisture–precipitation feedback. *Journal of the Atmospheric Sciences*, **71** (2), 782–799, <https://doi.org/10.1175/JAS-D-13-0180.1>, URL <https://journals.ametsoc.org/doi/10.1175/JAS-D-13-0180.1>.

Hagemann, S., and T. Stacke, 2015: Impact of the soil hydrology scheme on simulated soil moisture memory. *Climate Dyn.*, **44**, 1731–1750, <https://doi.org/10.1007/s00382-014-2221-6>.

Held, I. M., 2005: The gap between simulation and understanding in climate modeling. *Bull. Amer. Meteor. Soc.*, **86**, 1609–1614, <https://doi.org/10.1175/BAMS-86-11-1609>.

Hohenegger, C., P. Brockhaus, C. S. Bretherton, and C. Schär, 2009: The soil moisture–precipitation feedback in simulations with explicit and parameterized convection. *Journal of Climate*, **22** (19), 5003–5020, <https://doi.org/10.1175/2009JCLI2604.1>, URL <https://journals.ametsoc.org/jcli/article/22/19/5003/32298/The-Soil-Moisture-Precipitation-Feedback-in>.

- 579 Hohenegger, C., and B. Stevens, 2018: The role of the permanent wilting point in controlling the
 580 spatial distribution of precipitation. *Proceedings of the National Academy of Sciences*, **115** (22),
 581 5692–5697, <https://doi.org/10.1073/pnas.1718842115>, URL [https://www.pnas.org/content/115/](https://www.pnas.org/content/115/22/5692)
 582 [22/5692](https://www.pnas.org/content/115/22/5692).
- 583 Lynn, B. H., W.-K. Tao, and P. J. Wetzel, 1998: A study of landscape-generated
 584 deep moist convection. *Monthly Weather Review*, **126** (4), 928–942, [https://doi.org/](https://doi.org/10.1175/1520-0493(1998)126<0928:ASOLGD>2.0.CO;2)
 585 [10.1175/1520-0493\(1998\)126<0928:ASOLGD>2.0.CO;2](https://doi.org/10.1175/1520-0493(1998)126<0928:ASOLGD>2.0.CO;2), URL [https://journals.ametsoc.org/](https://journals.ametsoc.org/mwr/article/126/4/928/66256/A-Study-of-Landscape-Generated-Deep-Moist)
 586 [mwr/article/126/4/928/66256/A-Study-of-Landscape-Generated-Deep-Moist](https://journals.ametsoc.org/mwr/article/126/4/928/66256/A-Study-of-Landscape-Generated-Deep-Moist).
- 587 Manabe, S., 1969: CLIMATE AND THE OCEAN CIRCULATION: I. THE ATMOSPHERIC
 588 CIRCULATION AND THE HYDROLOGY OF THE EARTH'S SURFACE. *Monthly Weather*
 589 *Review*, **97** (11), 739–774, [https://doi.org/10.1175/1520-0493\(1969\)097<0739:CATOC>2.](https://doi.org/10.1175/1520-0493(1969)097<0739:CATOC>2.3.CO;2)
 590 [3.CO;2](https://doi.org/10.1175/1520-0493(1969)097<0739:CATOC>2.3.CO;2), URL [https://journals.ametsoc.org/view/journals/mwre/97/11/1520-0493_1969_097_](https://journals.ametsoc.org/view/journals/mwre/97/11/1520-0493_1969_097_0739_catoc_2_3_co_2.xml)
 591 [0739_catoc_2_3_co_2.xml](https://journals.ametsoc.org/view/journals/mwre/97/11/1520-0493_1969_097_0739_catoc_2_3_co_2.xml).
- 592 Peixóto, J. P., and A. H. Oort, 1983: The atmospheric branch of the hydrological cycle and
 593 climate. *Variations in the Global Water Budget*, Springer Netherlands, 5–65, [https://doi.org/](https://doi.org/10.1007/978-94-009-6954-4_2)
 594 [10.1007/978-94-009-6954-4_2](https://doi.org/10.1007/978-94-009-6954-4_2), URL https://doi.org/10.1007/978-94-009-6954-4_2.
- 595 Qian, J.-H., 2008: Why precipitation is mostly concentrated over islands in
 596 the maritime continent. *Journal of the Atmospheric Sciences*, **65** (4), 1428–
 597 1441, <https://doi.org/10.1175/2007JAS2422.1>, URL [https://journals.ametsoc.org/jas/article/65/](https://journals.ametsoc.org/jas/article/65/4/1428/26793/Why-Precipitation-Is-Mostly-Concentrated-over)
 598 [4/1428/26793/Why-Precipitation-Is-Mostly-Concentrated-over](https://journals.ametsoc.org/jas/article/65/4/1428/26793/Why-Precipitation-Is-Mostly-Concentrated-over).
- 599 Rodriguez-Iturbe, I., D. Entekhabi, and R. L. Bras, 1991: Nonlinear dynamics of soil moisture at
 600 climate scales: 1. stochastic analysis. *Water Resources Research*, **27**, 1899–1906, [https://doi.org/](https://doi.org/10.1029/91WR01035)
 601 [10.1029/91WR01035](https://doi.org/10.1029/91WR01035).
- 602 Schär, C., D. Lüthi, U. Beyerle, and E. Heise, 1999: The soil–precipitation feedback:
 603 A process study with a regional climate model. *Journal of Climate*, **12** (3), 722–741,
 604 [https://doi.org/10.1175/1520-0442\(1999\)012<0722:TSPFAP>2.0.CO;2](https://doi.org/10.1175/1520-0442(1999)012<0722:TSPFAP>2.0.CO;2), URL [https://journals.](https://journals.ametsoc.org/jcli/article/12/3/722/28833/The-Soil-Precipitation-Feedback-A-Process-Study)
 605 [ametsoc.org/jcli/article/12/3/722/28833/The-Soil-Precipitation-Feedback-A-Process-Study](https://journals.ametsoc.org/jcli/article/12/3/722/28833/The-Soil-Precipitation-Feedback-A-Process-Study).

606 Segal, M., and R. W. Arritt, 1992: Nonclassical mesoscale circulations caused by
 607 surface sensible heat-flux gradients. *Bulletin of the American Meteorological Society*,
 608 **73 (10)**, 1593–1604, [https://doi.org/10.1175/1520-0477\(1992\)073<1593:NMC CBS>2.0.CO;](https://doi.org/10.1175/1520-0477(1992)073<1593:NMC CBS>2.0.CO;2)
 609 2, URL [https://journals.ametsoc.org/view/journals/bams/73/10/1520-0477_1992_073_1593_](https://journals.ametsoc.org/view/journals/bams/73/10/1520-0477_1992_073_1593_nmccbs_2_0_co_2.xml)
 610 [nmccbs_2_0_co_2.xml](https://journals.ametsoc.org/view/journals/bams/73/10/1520-0477_1992_073_1593_nmccbs_2_0_co_2.xml).

611 Seneviratne, S. I., T. Corti, E. L. Davin, M. Hirschi, E. B. Jaeger, I. Lehner, B. Orlowsky, and
 612 A. J. Teuling, 2010: Investigating soil moisture–climate interactions in a changing climate:
 613 A review. **99 (3)**, 125–161, <https://doi.org/10.1016/j.earscirev.2010.02.004>, URL [https://www.](https://www.sciencedirect.com/science/article/pii/S0012825210000139)
 614 [sciencedirect.com/science/article/pii/S0012825210000139](https://www.sciencedirect.com/science/article/pii/S0012825210000139).

615 Sobel, A. H., C. D. Burleyson, and S. E. Yuter, 2011: Rain on small tropical islands. *Journal of*
 616 *Geophysical Research: Atmospheres*, **116**, <https://doi.org/10.1029/2010JD014695>, URL [https://](https://agupubs.onlinelibrary.wiley.com/doi/abs/10.1029/2010JD014695)
 617 agupubs.onlinelibrary.wiley.com/doi/abs/10.1029/2010JD014695.

618 Ulrich, M., and G. Bellon, 2019: Superenhancement of precipitation at the center of tropical islands.
 619 *Geophysical Research Letters*, **46 (24)**, 14 872–14 880, <https://doi.org/10.1029/2019GL084947>,
 620 URL <https://agupubs.onlinelibrary.wiley.com/doi/abs/10.1029/2019GL084947>.

621 Wang, S., and A. H. Sobel, 2017: Factors controlling rain on small tropical islands: Diurnal cycle,
 622 large-scale wind speed, and topography. *Journal of the Atmospheric Sciences*, **74 (11)**, 3515–
 623 3532, <https://doi.org/10.1175/JAS-D-16-0344.1>, URL [https://journals.ametsoc.org/jas/article/](https://journals.ametsoc.org/jas/article/74/11/3515/42168/Factors-Controlling-Rain-on-Small-Tropical-Islands)
 624 [74/11/3515/42168/Factors-Controlling-Rain-on-Small-Tropical-Islands](https://journals.ametsoc.org/jas/article/74/11/3515/42168/Factors-Controlling-Rain-on-Small-Tropical-Islands).

625 Zangvil, A., D. H. Portis, and P. J. Lamb, 1993: Diurnal variations in the water vapor bud-
 626 get components over the midwestern united states in summer 1979. *Interactions Between*
 627 *Global Climate Subsystems*, American Geophysical Union (AGU), 53–63, [https://doi.org/](https://doi.org/10.1029/GM075p0053)
 628 [10.1029/GM075p0053](https://doi.org/10.1029/GM075p0053), URL <https://onlinelibrary.wiley.com/doi/abs/10.1029/GM075p0053>.